Correlations in Nuclear Matter and Nuclei

F. Sammarruca[a], L. E. Marcucci[b,c], M. Viviani[c] and R. Machleidt[a]

[a] *Department of Physics, University of Idaho, Moscow, ID 83844, USA*
[b] *Dipartimento di Fisica "Enrico Fermi", Università di Pisa, Largo Bruno Pontecorvo 3, I-56127 Pisa, Italy*
[c] *Istituto Nazionale di Fisica Nucleare, Sezione di Pisa, Largo Bruno Pontecorvo 3, I-56127 Pisa, Italy*

Abstract

This contribution addresses momentum distributions in $A = 2, 3$ systems, with particular emphasis on high momentum components. The latter carry information on the short-range nuclear dynamics. We show predictions obtained with state-of-the-art chiral interactions and compare with those obtained with traditional, phenomenological or meson-theoretic, potentials. Model dependence is discussed, along with other aspects such as the impact of three-nucleon forces on the predictions.

Keywords: *Momentum distribution; short-range correlations; chiral nuclear interactions*

1 Introduction

The nuclear force has short-range repulsive and intermediate-range attractive components. Naturally, these features strongly limit the validity of a mean-field picture. Short-range correlations (SRC) refer to the nucleon dynamics at short distances and are responsible for the high-momentum components of nuclear wave functions.

An additional motivation for studying this important aspect of nucleon dynamics is provided by the lively experimental program aimed at extracting the SRC information via inclusive electron scattering at high momentum transfer or coincidence experiments involving knock-out of a nucleon pair [1–10].

In this contribution, we will first address high-momentum distributions and SRC in the deuteron, reviewing and updating one of our previous investigations [11]. We will then present a subselection of our most recent results [12] for momentum distributions and SRC in ^{3}He.

We conclude with some thoughts on the meaning and implications of measuring SRC. In future work, a careful consideration should be given to the approximations typically applied in order to extract the SRC information from high-momentum transfer electron scattering data.

Proceedings of the International Conference 'Nuclear Theory in the Supercomputing Era — 2018' (NTSE-2018), Daejeon, South Korea, October 29 – November 2, 2018, eds. A. M. Shirokov and A. I. Mazur. Pacific National University, Khabarovsk, Russia, 2019, p. 64.

http://www.ntse.khb.ru/files/uploads/2018/proceedings/Sammarruca.pdf.

2 High-momentum distributions in the deuteron

Deuteron momentum distributions in the context of SRC were studied in Ref. [11] using local and non-local realistic two-nucleon ($2N$) interactions. Those included: purely phenomenological local potentials, such as the Argonne v_{18} [13] (AV18) or the Nijmegen II [14] models, non-local meson-theoretic models, such as the charge dependent Bonn (CDBonn) potential [15], and state-of-the-art non-local chiral potentials [16–18]. In the study of Ref. [11], it was concluded that predictions of high-momentum distributions in the deuteron with non-local meson-exchange forces *or* state-of-the-art chiral forces are systematically lower than those obtained with the local AV18 or Nijmegen II potentials.

The analysis of Ref. [11] highlights non-localities in the tensor force as the source of differences in SRC among the various predictions. We recall that the presence of non-locality in the tensor force has been determined since a long time to be a desirable feature in nuclear structure calculations (see, for instance, Refs. [19–21].)

In Fig. 1 we show the deuteron momentum distributions $\rho(k)$, defined as the Fourier transform squared of the coordinate-space deuteron wave function. On the left side of the figure, we show the results, with focus on high-momentum components, obtained with the latest chiral interactions of Ref. [22] from the leading to fifth order ($\mathrm{N^4LO}$). On the right side of the figure, we show for comparison the same quantities calculated as in Ref. [11] with the older chiral potentials of Refs. [16–18]. We note that the convergence pattern shows improvement from the use of the new potentials.

We define the integrated probability of SRC in the deuteron as in Ref. [11], i. e.,

$$a_{2N}(d) = 4\pi \int_{k_{min}}^{\infty} \rho(k)\, k^2 dk, \tag{1}$$

where k_{min} is taken to be 1.4 fm^{-1}. This definition was adopted in Ref. [1], where the choice of the lower integration limit was suggested by the onset of scaling of

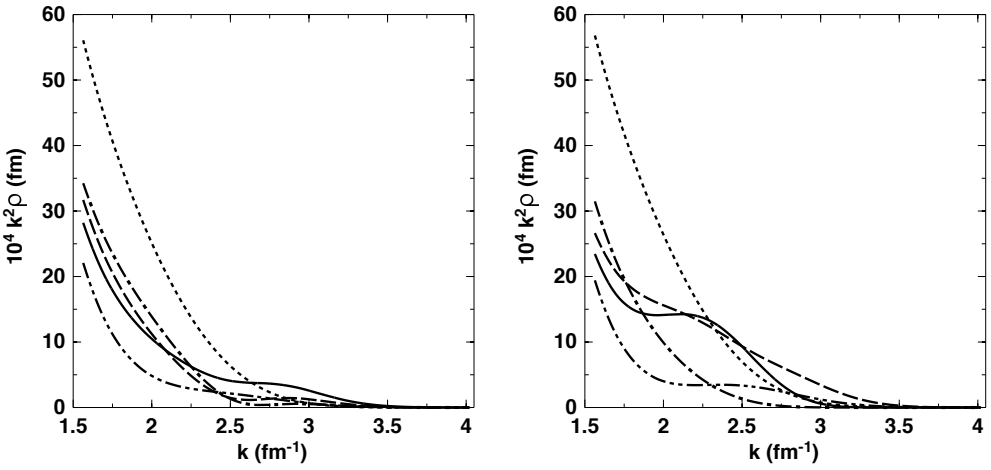

Figure 1: Left: Momentum distributions in the deuteron predicted with the chiral potentials of Ref. [22] at LO (dotted), NLO (dash-double dot), $\mathrm{N^2LO}$ (dash-dot), $\mathrm{N^3LO}$ (dash), $\mathrm{N^4LO}$ (solid). The cutoff is fixed at $\Lambda = 500$ MeV. Right: Predictions taken from Ref. [11] are obtained using the chiral potentials of Refs. [16–18].

Table 1: Probabilities of SRCs as defined in Eq. (1) and deuteron D-state percentage for the chiral interactions considered in the left panel of Fig. 1. The values in parenthesis, given for comparison, are taken from Ref. [11] and correspond to the distributions shown in the right panel of Fig. 1. The cutoff Λ is equal to 500 MeV in all cases.

Model	$a_{2N}(d)$	P_D
LO	0.046 (0.047)	0.0729 (0.0757)
NLO	0.015 (0.015)	0.0340 (0.0313)
N^{2}LO	0.026 (0.022)	0.0449 (0.0417)
N^{3}LO	0.024 (0.030)	0.0415 (0.0451)
N^{4}LO	0.024 (0.026)	0.0410 (0.0414)

electron scattering cross section, which should signal the dominance of scattering from a strongly correlated nucleon. The absolute per-nucleon SRC probability in a nucleus A can be deduced if the absolute per-nucleon probability in ^{3}He and the deuteron are calculated or estimated. More precisely,

$$a_{2N}(A) = a_2(A/^3\mathrm{He})\, a_{2N}(^3\mathrm{He}) \qquad \text{and} \qquad a_{2N}(^3\mathrm{He}) = a_2(^3\mathrm{He}/d)\, a_{2N}(d), \quad (2)$$

where $a_2(A_1/A_2)$ is the SRC probability for nucleus A_1 relative to nucleus A_2. The probability in the deuteron was taken to be equal to 0.041 ± 0.008 in Ref. [2]. We list in Table 1 the integrated probabilities $a_{2N}(d)$ defined in Eq. (1), calculated integrating the curves of Fig. 1 (left panel). As an additional, related information, we also show the corresponding D-state percentage. In fact, deuteron D-state probabilities are larger with stronger short-range central and tensor components of the nuclear force which, for the non-local chiral interactions and, generally, for non-local interactions, are softer than for the local AV18 potential. The values in parenthesis correspond to the distributions displayed on the right of Fig. 1, i. e., obtained with the older chiral potentials of Refs. [16–18]. As the table shows, there are huge variations between the LO and the NLO cases, and still large differences between the NLO and N^{2}LO. Variations at higher orders indicate a clear convergence pattern, definitely improved by the use of the newest potentials. Finally we notice that the deuteron integrated probabilities $a_{2N}(d)$ display significant model-dependence, as the corresponding values obtained with the AV18 and the CDBonn potentials are 0.042 and 0.032, respectively.

3 Momentum distributions in ^{3}He

In this Section, we show and discuss a subselection of results from Ref. [12] for momentum distributions in ^{3}He. We refer the reader to Ref. [12] for an extensive and detailed presentation of the formalism as well as additional predictions.

Note that the Hyperspherical Harmonics (HH) method is used to solve the $A = 3$ quantum mechanical problem. This method has the great advantage of being applicable in both coordinate- and momentum-space, with no restriction on the choice

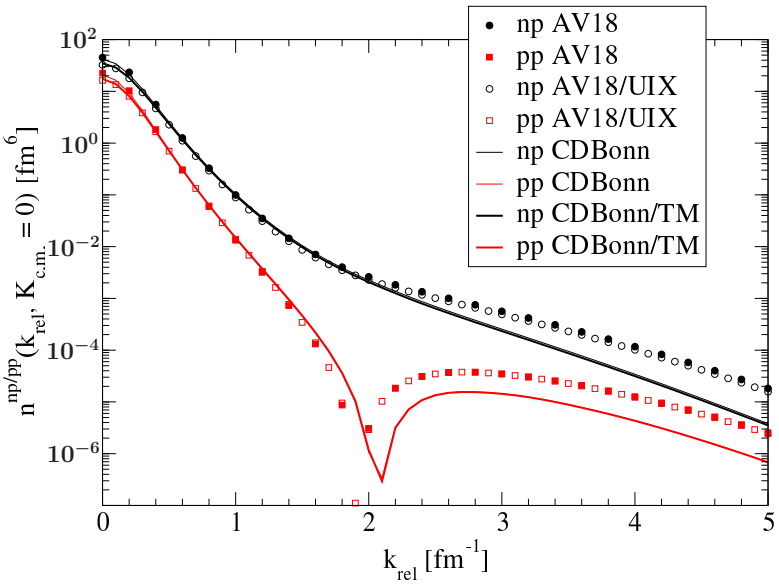

Figure 2: The $2N$ momentum distributions $n^{np/pp}(k_{rel}, K_{c.m.} = 0)$ in ^{3}He calculated using the AV18, AV18/UIX, CDBonn and CDBonn/TM $2N$ and $3N$ interaction models. The thin and thick lines essentially overlap.

of the nuclear potential model, which can be local or non-local. The starting point are the so-called Jacobi coordinates, which are defined in the coordinate space as in Refs. [23, 24].

We first explore the model-dependence of the $2N$ momentum distributions, by comparing predictions based on the CDBonn potential without or with the Tucson–Melbourne (TM) [25] three-nucleon ($3N$) force with those based on the AV18, without or with the UIX $3N$ force [26]. In Fig. 2 we show results for the $n^{np/pp}(k_{rel}, K_{c.m.} = 0)$, namely, we have selected the "back-to-back" (BB) configuration for the nucleon pair. We observe that the results with CDBonn/TM and those with AV18/UIX are substantially different from each other, especially in the high-k_{rel} tails, confirming consistency with our earlier observations about the deuteron. Furthermore, the $3N$ force contributions are barely appreciable on the logarithmic scale of the plot.

We now turn our attention to the $2N$ momentum distributions obtained with the $2N$ chiral potentials without or with the $3N$ forces, obtained as discussed in Ref. [12]. We begin with studying the order-by-order pattern, using the $\Lambda = 500$ MeV cutoff as an example. The results obtained with the other values of Λ display a similar behavior. In Fig. 3 we show the BB np momentum distribution $n^{np}(k_{rel}, K_{c.m.} = 0)$ obtained using only the $2N$ force at LO, NLO, N2LO, N3LO and N4LO. The figure reveals that the LO curve has a distinctly different behavior at small k_{rel} compared with the other curves, which suggests that the asymptotic part of the wave function at LO is significantly different than at the higher orders. Figure 4 displays the same predictions but for the pp pair, also BB. As we can see, similar remarks apply to the pp case as well. We also observe that the N3LO and N4LO curves are very similar up to $k_{rel} \simeq 2.2$ fm^{-1}, indicating satisfactory order-by-order convergence at least in the region where the distributions still have non-negligible size.

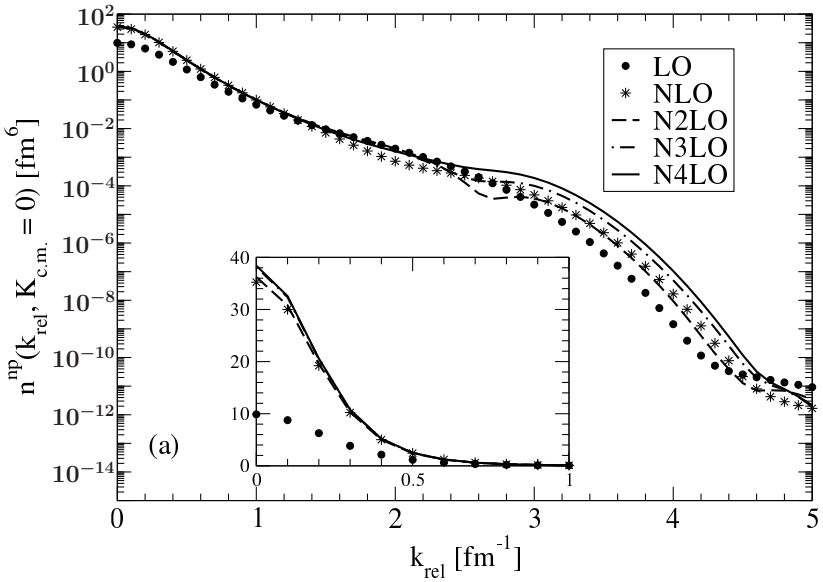

Figure 3: The np momentum distributions $n^{np}(k_{rel}, K_{c.m.} = 0)$ in ^{3}He calculated using only $2N$ chiral interactions with $\Lambda = 500$ MeV. The different chiral orders are labelled as in the text. In the inset we show the small k_{rel} range ($k_{rel} \leq 1$ fm^{-1}) on a linear scale.

The BB $2N$ momentum distributions $n^{np}(k_{rel}, K_{c.m.} = 0)$ and $n^{pp}(k_{rel}, K_{c.m.} = 0)$ calculated with and without $3N$ interaction, at different chiral order and for different values of the cutoff Λ, are shown in Figs. 5 and 6, respectively. The cutoff dependence is negligible below $k_{rel} \simeq 2.2$–2.5 fm^{-1}, and increasingly strong above that.

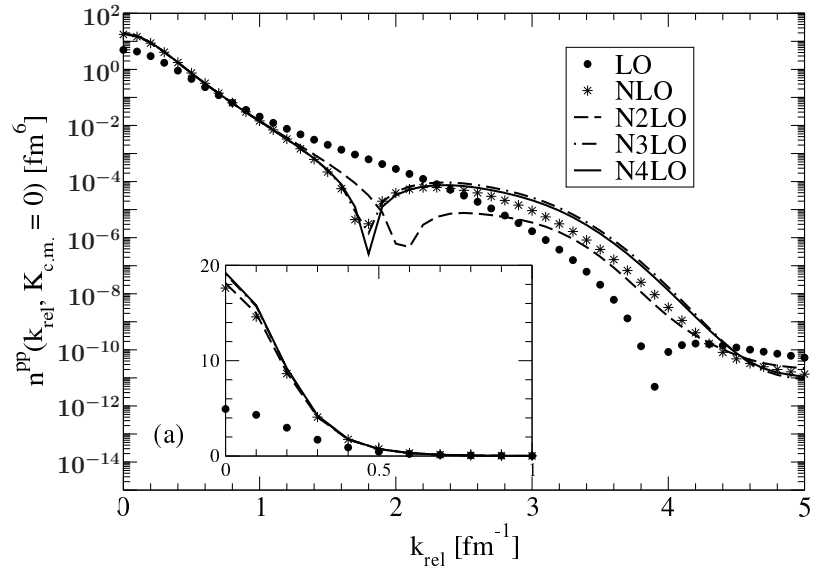

Figure 4: Same as Fig. 3 but for the pp pair.

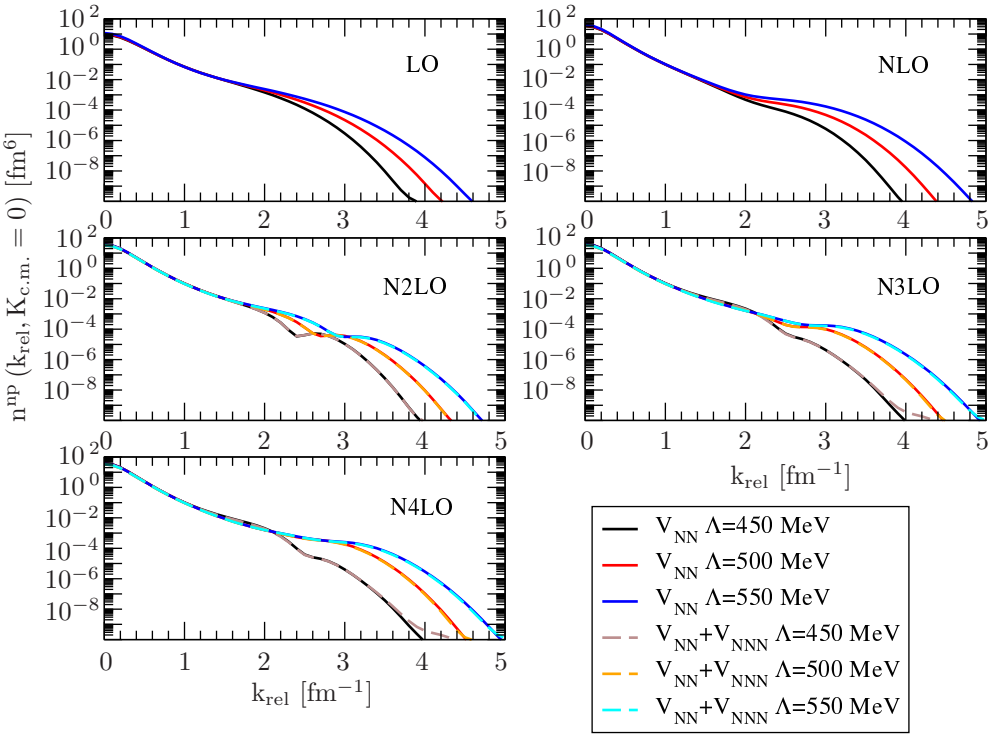

Figure 5: The np momentum distributions $n^{np}(k_{rel}, K_{c.m.} = 0)$ in ^{3}He calculated using only $2N$ (solid lines) and $2N+3N$ (dashed lines) chiral interactions, at different chiral order and for three values of the cutoff $\Lambda = 450, 500, 550$ MeV. In all panels, the lines from bottom to top correspond to the lower to higher values of Λ. Our approach to the construction of the leading $3N$ force is described in Ref. [12].

Furthermore, the $3N$ force contributions are visible only for $k_{rel} \geq 3.0{-}3.5$ fm^{-1}. Note, however, that above $k_{rel} \simeq 2.5$ fm^{-1} all momentum distributions are so small that the differences are of no practical relevance.

As noted for the deuteron case, the momentum distributions calculated with chiral interactions die out at a faster rate than those obtained with phenomenological potentials, a feature which may be expected given the softer nature of chiral forces. While this is a correct observation within the spectrum of interactions considered here, it is important to note that the chiral nature of an interaction does not necessarily bring the additional softness. To support this statement, we refer to Ref. [27], where predictions for single-nucleon and $2N$ momentum distributions in $A \leq 16$ are shown. In that work, it is concluded that, when *local* chiral interactions are employed, the resulting momentum distributions are *consistent* with those obtained from local phenomenological potentials. In fact, the local $2N$ chiral interactions (at N2LO) applied in Ref. [27] and developed in Refs. [28, 29] predict a D-state probability for the deuteron ranging between 5.5 and 6.1%, values which are typical for the "hardest" local potentials.

Therefore, once again, the local vs non-local nature of the $2N$ force (by far the largest contribution to our predicted momentum distributions), is a major factor in

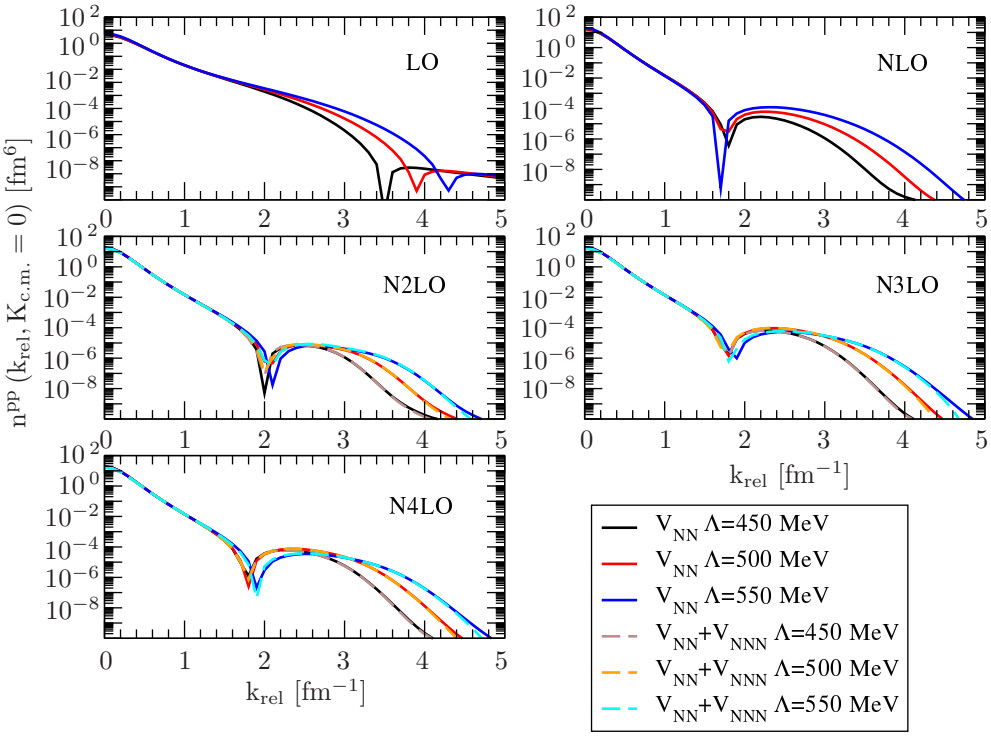

Figure 6: Same as Fig. 5 but for the *pp* pair.

determining the theoretical momentum distributions in nuclei and, particularly, their short-range part.

4 Conclusions and outlook

We have discussed predictions for the $2N$ momentum distributions in the deuteron and ^{3}He. Our predictions are based on the state-of-the-art chiral $2N$ potentials, including (or not) the leading chiral $3N$ force. Also, for the purpose of comparison, we have considered older potentials plus an appropriate $3N$ force, either fully phenomenological or based on meson theory. One of the main motivations was to explore the short-range few-nucleon dynamics as predicted by these diverse interactions. One of our findings is that, regardless the $2N$ force model, the contribution from the $3N$ forces is weak.

We find a significant model dependence, especially in the high-momentum tails of the momentum distributions, with both phenomenological and chiral potentials. We have explored the cutoff dependence and found that it can be significant. This is the case, though, in the region where the momentum becomes larger than the cutoff values themselves.

Although potentials based on chiral EFT may be expected to produce weaker SRC than purely phenomenological or meson-exchange ones, the local vs non-local nature of the underlying $2N$ force appears to be a major factor in the observed model dependence. We find this to be an important issue, extensively debated in

the literature of the 1990's [19–21] and now re-emerging along with new stimulating discussions around electron scattering measurements.

The $2N$ potentials considered here have an established success record with low-energy predictions, such as the structure of light and medium-mass nuclei as well as the properties of nuclear matter. But, as shown above, they differ considerably in their high-momentum components. Note that there is no physical reason why the off-shell behavior of, say, AV18, should be preferable as compared to other potentials. In fact, on the fundamental grounds, the off-shell behavior is not an observable. High momentum transfer reactions are easier to analyze using one-body currents of the impulse approximation, suitable with harder $2N$ potentials, whereas the use of soft, non-local potentials, complicates the currents necessary to describe high momentum transfer experiments [30]. One should carefully consider, for instance, to which extent analyses of quasielastic electron scattering in terms of external radiation graphs [30], without gauge-invariance preserving terms, may cause a sensitivity to the (otherwise unobservable) off-shell behavior.

Acknowledgments

The work of F.S. and R.M. was supported by the U.S. Department of Energy, Office of Science, Office of Basic Energy Sciences, under Award Number DE-FG02-03ER41270. Computational resources provided by the INFN-Pisa Computer Center are gratefully acknowledged.

References

[1] K. S. Egiyan *et al.*, Phys. Rev. Lett. **96**, 082501 (2006) *and references therein.*

[2] K. Sh. Egiyan *et al.*, CLAS-NOTE 2005-004 (2005), https://misportal.jlab.org/ul/physics/Hall-B/clas/index.cfm?note_year=2005.

[3] K. Sh. Egiyan *et al.*, Phys. Rev. C **68**, 014313 (2003).

[4] M. McGauley and M. M. Sargsian, arXiv:1102.3973v3 [nucl-th] (2012).

[5] E. Piasetzky, M. Sargsian, L. Frankfurt, M. Strikman and J. W. Watson, Phys. Rev. Lett. **97**, 162504 (2006).

[6] A. Tang *et al.*, Phys. Rev. Lett. **90**, 042301 (2003).

[7] I. Korover *et al.* (Jefferson Lab Hall A Collaboration), Phys. Rev. Lett. **113**, 022501 (2014).

[8] R. Shneor *et al.* (Jefferson Lab Hall A Collaboration), Phys. Rev. Lett. **99**, 072501 (2007).

[9] R. Subedi *et al.*, Science **320**, 1476 (2008).

[10] H. Baghdasaryan *et al.* (CLAS Collaboration), Phys. Rev. Lett. **105**, 222501 (2010).

[11] F. Sammarruca, Phys. Rev. C **92**, 044003 (2015).

[12] L. E. Marcucci, F. Sammarruca, M. Viviani and R. Machleidt, Phys. Rev. C **99**, 034003 (2019).

[13] R. B. Wiringa, V. G. J. Stoks and R. Schiavilla, Phys. Rev. C **51**, 38 (1995).

[14] V. G. J. Stoks, R. A. M. Klomp, C. P. F. Terheggen and J. J. de Swart, Phys. Rev. C **49**, 2950 (1994).

[15] R. Machleidt, Phys. Rev. C **63**, 024001 (2001).

[16] D. R. Entem and R. Machleidt, Phys. Rev. C **68**, 041001(R) (2003).

[17] E. Marji, A. Canul, Q. MacPherson, R. Winzer, Ch. Zeoli, D. R. Entem and R. Machleidt, Phys. Rev. C **88**, 054002 (2013).

[18] R. Machleidt and D. R. Entem, Phys. Rep. **503**, 1 (2011).

[19] R. Machleidt, F. Sammarruca and Y. Song, Phys. Rev. C **53**, R1483(R) (1996).

[20] A. Polls, H. Müther, R. Machleidt and M. Hjorth-Jensen, Phys. Lett. B **432**, 1 (1998).

[21] H. Müther and A. Polls, Phys. Rev. C **61**, 014304 (1999).

[22] D. R. Entem, R. Machleidt and Y. Nosyk, Phys. Rev. C **96**, 024004 (2017).

[23] M. Viviani, L. E. Marcucci, S. Rosati, A. Kievsky and L. Girlanda, Few-Body Syst. **39**, 159 (2006).

[24] A. Kievsky, S. Rosati, M. Viviani, L. E. Marcucci and L. Girlanda, J. Phys. G **35**, 063101 (2008).

[25] S. A. Coon and H. K. Han, Few-Body Syst. **30**, 131 (2001).

[26] B. S. Pudliner, V. R. Pandharipande, J. Carlson and R. B. Wiringa, Phys. Rev. Lett. **74**, 4396 (1995).

[27] D. Lonardoni, S. Gandolfi, X. B. Wang and J. Carlson, Phys. Rev. C **98**, 014322 (2018).

[28] A. Gezerlis, I. Tews, E. Epelbaum, S. Gandolfi, K. Hebeler, A. Nogga and A. Schwenk, Phys. Rev. Lett **111**, 032501 (2013).

[29] A. Gezerlis, I. Tews, E. Epelbaum, M. Freunek, S. Gandolfi, K. Hebeler, A. Nogga and A. Schwenk, Phys. Rev. C **90**, 054323 (2014).

[30] O. Hen, G. A. Miller, E. Piasetzky and L. B. Weinstein, Rev. Mod. Phys. **89**, 045002 (2017).